Semi-Annual Status Report

November, 1966

NASA Grant NGR-10-007-028 (Supplement #1)

REPORT ON LASER BACK-SCATTER SYSTEM AND SUBSYSTEMS

submitted to

Office of Space and Applications
National Aeronautics and Space Administration
Washington, D. C.

by

School of Environmental and Planetary Sciences
University of Miami
Coral Gables, Florida

Prepared by _____
Luis M. Herrera-Cantilo
Project Director

Approved by _____
S. Fred Singer
Principal Investigator

TABLE OF CONTENTS

LIST OF FIGURES

November 1966

NASA GRANT NGR-10-007-028 (Supplement #1)

1. Introduction

In the first phase of this project, the feasibility of a scattering experiment was examined, whereby a laser beam would be directed at the zenith and the back-scatter from it detected at the ground and analyzed. The beam being pulsed, ranging could be done and so, by also measuring the intensity of the backscatter, information could be otained on:

a) The number density of the atmosphere as a function of height, up to about 80 km.

b) The presence and height of possible dust layers and their average backscattering cross-section per unit volume. For concentrations of 10 particles per cubic meter and particle radii of 1 micron, this would be possible up to altitudes of about 100 to 150 km, depending on system parameters.

It was further shown that the information would have to be retrieved statistically, by summing the returns of many successive laser shots and that the system component that would have the greatest influence in the number of shots required was the mirror of the receiving telescope. For a high-quality mirror, a very small field of view could be accurately determined, which would minimize the interference from sky-background radiation; while a mirror of large size would maximize the amount of back-scattered radiation received.

It was finally pointed out that, for a given cost of mirror, its size and quality tend to be mutually exclusive and that a trade-off had to be reached. Calculations indicate that size is actually more effective than quality in reducing the number of shots required. However, a mirror of the minimum acceptable quality and large size is not available at present and not easy to come by; results were, therefore, worked out also for an astronomical mirror that is on hand, and it was indicated that it would be used in the first period of the observations.

2. General Description of the System

Figure 1 shows the general layout, built around the 18" reflecting telescope in our astronomical observatory at West Palm Beach.

The laser is to be installed in an enclosed extension added to the main dome. In the figure, (1) is the Q-spoiled laser, (2) is the cabinet containing the power supply and discharging circuits, and (3) is a fast shutter intended to prevent the transmission into the atmosphere of the fluorescence emitted by the laser after the main pulse. The main pulse is repeated once per second.

A light-pipe (4) enters the dome and, by means of suitable lenses, spreads the beam over the secondary mirror of the transmitting telescope (5). This is mounted piggy-back on the receiving telescope. Therefore, both telescopes move together without change in the angle between their axes, which makes it easy to align the system by tracking a star.

The backscattered light is received in the main telescope (6), at whose output point is located a box (7), that we designate as the optical receiver. It intercepts, collimates, and filters the beam from the telescope. It also includes another fast shutter used for high-altitude observations in order to prevent the intense backscatter from the troposphere from reaching the detector, where it would produce a noise condition of long duration.

A light-pipe (8) channels the received radiation into the detector (9). This is an EMI 9558 QA photomultiplier, cooled by a continuous flow of cold nitrogen gas which is recirculated through a cooling agent in the tank (10) by a pump (11). The quantum detective effeciency of the phototube is artificially

increased by making use of several successive reflections of the beam within the quartz window of the tube. This necessitates introduction of the light at an angle of about 45^{o} to the tube axis, which is the reason why the whole detector case sits on a 45^{o} ramp.

The output of the phototube is amplified in a vacuum-tube preamplifier (12), mounted onto the detector case. Signals are then applied to a video-amplifier (13), which includes a precise tunnel-diode threshhold-detector, thus minimizing the probability of counting dynode-generated noise pulses.

A timing unit (14), synchronized by the laser pulse, generates a raster whose duration and delay relative to the trigger are both adjustable in steps. Range markers are also generated. They are mixed with the video signals in the display unit (15) and presented on the raster in a 7" CRT. A photographic camera (16) serves to superimpose a large number of successive scans in a time-integrated record. A separate but identical CRT provides direct observation of successive individual scans.

3. Detailed Description of the System

3.1 The Transmitter

The laser used in this transmitter is a product of Applied Lasers, Inc. of Stoneham, Massachusetts. It consists of a model 1010 C2 laser head, which is essentially a dual split elliptical cavity, where a $6\frac{5}{8}'' \times \frac{5}{8}''$ ruby rod is excited by two FX47b flash lamps. The ruby and flash lamps are cooled by a self-contained recirculating water system, where the water is in turn cooled in a refrigerating unit. The operating wavelength is 6943 Å.

The Q-spoiling is done by a combination of a rotating prism and a saturable cell, the former being controlled by a 400 c/s power supply, whose phase is adjustable with respect to the flash-lamp waveform.

A separate cabinet houses the power supply and the 1500 microfarad condenser bank for the operation of the flash lamps, as well as the main controls and indicators. It requires a 220 v three-phase supply.

The laser is capable of three modes of operation; namely, without the Q-switching unit, with all of it, or with the rotating mirror only. In the first mode, it generates pulses of about 50 joules, once per second, with a duration close to one millisecond. With the complete Q-switching attachment, single-spike pulses of about 30 nanoseconds and 7 joules are produced at the rate of one per second. In this experiment, however, it will be operated mainly without the saturable cell. In this mode, it produces pulses of about 5 microseconds

with a jagged envelope that may be regarded as a train of overlapping spikes. Their energy content, at the rate of one per second, is about 10 joules. A further improvement in the performance is brought about by the use of an external sapphire front reflector.

A photodiode and associated circuit is provided to pick up some light scattered out of the beam at an optical surface such as a lens. The pulse thus obtained serves two important purposes. First, it provides synchronism to the timing unit, where it becomes the zero of the range scale. Secondly, it is used in conjunction with a vacuum-tube voltmeter to provide relative pulse-energy readings. The system is periodically calibrated with a liquid-cell calorimeter whose accuracy, however, is limited to about 10%.

3.2 The Fluorescence Shutter

Figure 2 shows, on a qualitative amplitude scale, the time relationship between the flash-lamp current wave (dashed curve), the fluorescence emission from the ruby (full curve) and the correct timing of the prism; i.e., the laser pulse, just before the peak of the fluorescence (shown by arrow).

Since the whole ranging process through 150 km of atmosphere lasts 1 millisecond, starting at the arrow, it is clear that much light from this fluorescence will be scattered into the receiver during the whole cycle if it is allowed to reach the atmosphere at all.

The only way to prevent this is to separate the laser from the atmosphere by a fast shutter, capable of opening only during a very short time, of the order of the duration of the pulse itself, say, 10 microseconds. Furthermore, this shutter should have a very short opening time (about 1 microsecond) and must be very accurately timed to the laser.

Rotating shutters have been used in this connection, geared to the rotating prism. Although they do the job, their transition from the closed state to the completely open state tends to be somewhat slow in comparison to the pulse duration. As a result, the light pulse is actually shaped by the shutter, whence an uncertainty in the effectively transmitted energy.

In this experiment, a different type of shutter, in principle capable of very fast transitions, is under development for use in the receiver; it may also be used here if its performance indeed meets the requirements. This is, however, still open to question and a rotating shutter may still be used, either permanently or until the other type is ready. The other kind of shutter is discussed in conjunction with the receiver (see 3.5).

3.3. Transmitter Output

Problems related to the coupling of the intense flash-lamp pulse into all neighboring circuits have made it advisable to install the laser in a metallic and grounded enclosure erected against the dome, on the outside. The laser beam will then be directed to the transmitting telescope by means of a

4m long light-pipe. As transmitting telescope, we plan to use our 6" reflector which has a focal length of 48". The beam will almost certainly be collimated after the laser or shutter.

The transmitting telescope will be mounted on the side of the receiving telescope, so that both will track together. The optical axes of both telescopes being about 40 cm apart, and since the receiving field of view is going to be limited by a focal-plane stop, also to 1 milliradian, it is concluded that, when aligned at infinity, both beams will start to overlap at a height of about 400 m, and that at a height of about 4000 m, 90% of their diameters will overlap.

With this arrangement, then, the boresighting problem is essentially removed, the fields of both telescopes overlap continuously from a very low altitude, and still the laser is removed far enough to avoid troubles arising from its proximity to the receiver.

3.4 Receiving Telescope and Optical Receiver

This is a Newtonian-type telescope based on an 18" astronomical mirror, which has a 148" focal length. It will be made to track during the alignment of the transmitting telescope, but for the rest of the experiment, it will be fixed and pointed at the zenith.

The optical receiver is a light-tight box that will be mounted in place of the eye-piece. It is still under development, and Figure 3 shows its preliminary design. At left is the main telescope; the dotted line shows the axis

of the beam coming from the secondary mirror of the telescope. Number 1 designates an X-Y-Z mount supporting the aperture stop (2) and collimating lens (3). The latter must have its focus in the opening of the aperture stop, and is pre-adjusted on the mount to that effect. The object of the mount is to position these two elements so that the beam of the telescope also comes to focus in the opening of the stop, once the whole receiver has been bolted in place. Mounted in fixed positions are two filter holders (4), one of them holding an interference filter whose pass-band is centered at 6942 Å, with a half-power bandwidth of 19 Å and a peak transmission of 78%. This filter was acquired from Baird Atomics, Inc.

Number 5 designates the high-speed shutter, discussed in more detail below. It really acts as a switch, so that it either deflects the incoming light downward, through the outlet (6) that leads into the light-pipe, or lets it out along a straight path, through the opening (7), where an eye-piece could again be installed.

The operational output of the optical receiver, through the opening (6), will then be a parallel filtered beam of light, of a diameter of about 0.5 centimeters, consisting of backscatter from the laser beam, which fills the field of view, plus whatever sky background passes through the filter window.

3.5 The Proposed High-Speed Shutter

It was shown in our previous Semi-Annual Report (March 1966) that, due to the considerable increase of atmospheric density with decreasing

altitude, the backscattering cross-section would be greater at sealevel than at a height of 100 km, by a factor of about 2 million. The factor is even greater in practice, considering the amount of particulate matter suspended at low altitudes. In fact, it was learned from a similar project (R. Wright, private communication), that the intense backscatter from the lower layers could be sufficient to establish in the photomultiplier a noise condition that would persist for more than a millisecond and obscure the returns from the high atmosphere.

In order to avoid this perturbation, it is advisable to protect the phototube with a shutter during the transit of the laser beam through the troposphere, at least when high-altitude observations are in progress and the system is used at maximum sensitivity. (When observing the lower atmosphere, since the backscatter is so intense, the phototube can be permanently protected by a neutral filter - thus the second holder in the optical receiver - and the shutter is not needed.)

The display of high-altitude observations starts at a height of 60 km as will be seen when discussing the timing and display units; in other words, 400 microseconds after the laser pulse is fired. The shutter should remain closed most of that time and start opening, say, after 350 microseconds (when there would be a timing pulse available). That leaves 50 microseconds to open it - a rather short time for a mechanical shutter.

It is then proposed to build a shutter on a principle that has been applied to the construction of a Q-switch for a laser, namely, frustrated total

internal reflection.[1] The principle is illustrated in Fig. 4. Consider a beam of light coming from the left into prism A, made of a material such that its minimum angle of total reflection is less than 45°. Then, upon hitting the hypotenuse, the light beam is totally deflected 90°, in this case downwards (dot-dash line). If, however, another prism B, of the same material is brought into optical contact with prism A, the optical discontinuity effectively disappears and the beam goes straight through (dotted line). A quantitative theory is now available for the intensities of the various rays (reflected, refracted and evanescent) as a function of the separation between both prisms.[2] It turns out that for separations down to one-twentieth of a wavelength, 98% of the light goes through, while for separations of at least one wavelength, 98.3% of the light is reflected.

The problem at hand now is how to move prism B against and away from prism A. One possible answer, which has been described by I. Court and K. Von Willisen and is now being tested in our laboratory, is the use of piezoelectric ceramics, which, under voltage pulses of a few hundred volts, are capable of contractions or expansions of the order of a micron with considerable force. Also, proper design of the ceramic transducer makes it adaptable to almost any frequency response, thus permitting the excursion to take place in a few microseconds.

The necessary piezoelectric ceramics are available in a wide range of shapes, sizes, and responses from the Clevite Corp., Cleveland, Ohio; we are at present working with a few samples acquired from them.

---

[1] I Court and K. Von Villisen, Applied Optics, Vol 3, No. 6, pp 719 (June, 1964).

[2] La reflexion vitreuse, H. Arzelies, Annales de Physique, I, p. 5, 1946.

However attractive, this scheme still presents a few experimental difficulties, and we may begin our observational program with a shutter of more conventional design. If, however, it proves successful in reasonable time, then we plan to use the frustrated reflection shutter, both in the optical receiver and in the transmitter, as indicated above.

3.6 The Detector Sensitivity Improvement

The choice of a suitable photomultiplier was discussed in our previous Semi-Annual Report (March 1966). It was shown that two characteristics of the tube are prominent as system parameters; namely, the quantum efficiency and the dark current; and that in the overall result, the former prevails. Accordingly, our choice was the tube with the highest quantum efficiency (5.3%) the RCA C70038D.

However, it was brought to our attention at the time that the detective efficiency of a phototube can be "artificially" increased by introducing the beam into it at an angle, to the window, greater than that of total reflection. If, now, the window is a plane-parallel plate, the beam will be guided within this plate and will undergo successive total reflections at both faces. However, the photocathode is painted on one of these faces; every time the beam hits it, photoelectric action will take place and some photoelectrons will be released. In the end, their total number will be appreciably greater than that obtained by the usual single axial traverse of the window. The effect is wavelength dependent

and the gain for red light is about 4.[3] The possibility of this improvement has a bearing on our choice of tube. To make this clear, let us review some information on commercially-available phototubes, as summarized in the following table:

Manufacturer	Type	Quantum Efficiency	Dark Count (uncooled)*	Window Shape
RCA	C70038D	5.3%	2.1×10^5	Dormer, curved cathode
RCA	8644	2.5%	3.6×10^4	Plano-spherical
RCA	7265	2.5%	1.9×10^5	Plano-curved
EMI	9558QA	2.5%	4.4×10^3	Plane-parallel
EMI	9529	1.0%	7.5×10^3	Plane-parallel
ITT	FW-130	2.5%	7.8×10^4	Plano-spherical
ITT	F-4003	2.5%	125	Plano-spherical

* The dark count given here is the cathode dark-current given by the manufacturer, divided by the charge of the electron, in counts/sec.

These are the phototubes that we considered in our previous semi-annual report when we made our selection. We then selected the first, on account of its high quantum efficiency.

However, the total internal reflection method cannot be used with the C70038D, because of the peculiar geometry of its window and cathode. In fact, it is seen from the Table that only the two EMI tubes are suitable for that improvement, since a plane-parallel window is a requirement, as pointed out above.

It is clear, then, that the EMI9558QA is the best choice, since its quantum efficiency can be brought to about 10% for red light - a twofold

[3] See, for instance, "Enhancement of Photomultiplier Sensitivity by Total Internal Reflection," W. D. Gunter, et al, Applied Optics, IV, p. 512-13, April 1965.
Also, "High Absolute Photocathode Sensitivity," G. R. Grant, et al, Rev. of Scientific Instruments, X, p. 1511-12, October 1965.

improvement over the C70038D. Also, the 9558QA is one of the least noisy tubes listed. And, last but not least, it has a large cathode (2" in diameter) which makes it particularly convenient for the proposed technique. Accordingly, we acquired one photomultiplier of this type.

The method is illustrated in Fig. 5. The prism used to provide a front surface normal to the beam is in optical contact with the window, as indicated by the dotted line. Thus, the beam - here represented by its axis - enters the window at point P without reflection and proceeds to reach the photocathode at point R. Most of the light, however, is reflected there (totally, if the angle is adequate) and returns to the front face, where it is again reflected at point Q. Photoelectrons are produced at points such as R and S, as the beam travels across the tube face.

The angle of incidence of the beam with respect to the tube face must be greater than the minimum angle for total reflection, given by arc sin (1/n), where n is the refractive index of the window. It should not be much greater, however, because then the number of bounces across the tube face would be reduced and eventually even the photoelectric reaction would lose efficiency. It turns out that for the window of the 9558QA, an incidence angle of 45^{o} is adequate, whence the 45^{o} - 90^{o} - 45^{o} prism shown in Fig. 5.

The thickness of the window poses another problem. For incidence at 45^{o}, the distance between the point of entry into the window and the first reflection at the front face - points P and Q in the figure - is equal to 2D, where

D is the thickness. Now the prism cannot be permitted to extend over point Q, because the light would then enter the prism again at Q and leave the system forever through the opposite face of the prism. In other words, there is a definite upper limit to the size of the prism; its hypotenuse must be smaller than 2D, therefore, the sides of its right angle must be shorter than 1.4D or, if the prism is larger, only a strip of width 1.4D along its right angle can be used for light input.

Now, the 9558QA has a window thickness of some 2mm, which means that the cross-section of the beam is limited to 2.8mm - a rather small value. However, it is not advisable to alleviate this problem by increasing the window thickness (by means of a parallel plate added on the face) because this would reduce the number of bounces and would therefore be self-defeating. Instead, the beam will be brought to focus at point R (Fig. 5) by means of a single lens built into the detector case.

This, of course, makes the beam convergent, and all the light in it should still impinge on the tube face at an angle that will produce total reflection. In this regard, the value of 45°, indicated above, leaves room for a cone of about 3° half angle. We start from a parallel beam of about 0.5 cm cross-section and will use a lens of about 2 cm focal length to focus the beam of point R.

3.7 The Detector Housing

Dark current in photomultipliers can be reduced by a factor as great as 1000 by cooling their cathode. For S-20 photocathodes, it seems

sufficient to reach temperatures of the order of -40^{o} C. No improvement results from further cooling. Since, however, it is difficult to ascertain the actual temperature of the cathode, it is customary to operate at lower temperatures as a safety measure. Cooling agents in frequent use are dry ice and cold nitrogen, either liquid or gaseous.

We chose the latter in this case, mainly for simplicity and flexibility in operation. On this basis, the enclosure shown in Fig. 6 was designed, taking also into account other objectives such as light-tightness, ease of optical adjustment, and ease of assembly.

The outer case, roughly 17" x 11" x 11", is being made in welded aluminum by a local commercial workshop. We built into it a lining of polystyrene-type insulation, 4" thick, that forms a cylindrical cavity in the center, of a diameter of about 3". The figure shows, in the middle, the photomultiplier (A) with its socket and prism. Around it goes a cylindrical electrostatic-magnetic shield (B), acquired from the Perfection Mica Company, Magnetic Shield Division, Chicago, Illinois. The shield supports the lens holder (C), referred to in the previous section. The light beam enters the box through a nylon tube (D), closed at both ends with optical flats and filled with dry nitrogen. The outer coupling connects to the light pipe (8, in Fig. 1).

The photomultiplier socket is actually fastened to the shield, in which it can be adjusted back and forth with appropriate screws. By referring

to Fig. 5, it is seen that this amounts to sliding point R up and down along the photocathode. On the other hand, the lens also screws in and out along its holder, thereby providing a focus adjustment. Both adjustments are meant to be preset in the laboratory, whereupon the shielded-tube assembly slides into place in the cavity (which opens at the rear) and is screwed to some nylon structure embedded in the insulation and tied to the outer box.

Now the box is clamped onto the 45^{o} ramp (see Fig. 1) and connected to the cooling circuit. In Fig. 6, the gas intake is shown at (E), blowing cold nitrogen on the face of the tube. The nitrogen then flows around the tube in the shield, out at the back, and forward around the shield, and finally reaches the outer chamber (F), which surrounds the enclosure and from which it is extracted at (G).

It is intended to operate the system in the recirculating mode, for greater economy. A suitable pump (11, in Fig. 1) will force the gas from the detector box into a cooling tank (19, in Fig. 1), where it will be refrigerated in dry ice, and back to the detector. The package is, however, easily convertible to use of evaporating nitrogen (as reported, for example, by R. Wright), should this change seem advisable.

The dynode resistors are of the very small metal oxide type and are mounted on the socket. One connection brings the necessary high voltage from a pack of batteries. Batteries were chosen here in order to avoid any possible coupling of the laser pulse to the detector through the mains. The photomultiplier

will be operated under a total voltage of 900 v, a comparatively low value, in order to help minimize dark current.

A second connection brings the anode signal out to the preamplifier (12, in Fig. 1).

3.8 The Preamplifier

For the application described, the preamplifier design was straightforward. Since it was desired that every electronic event be detected, straight video techniques were used. And since the signal-to-noise ratio of such electronic events is very high, no special circuit precautions were necessary. The evolved design took advantage of the simplicity of shunt-peaked vacuum tube circuiting, and the compactness of having the vacuum tube be a pentode-dual triode. The pentode stage provides high gain for the $< 0.1\,\mu$ second pulses from the photomultiplier. The second triode stage provides pulse inversion and some gain for the final cathode follower stage. Speaking of performance, a gain of 50 for the $< 0.1\,\mu$ second pulse is achieved, resulting in a gain-bandwidth product of over 500 mc. The circuit appears in Fig. 7.

3.9 Video Amplifier and Threshhold Detector

The ensuing video amplifier was designed to provide gain while maintaining pulse shape. Gain was needed to drive the threshhold circuit, while pulse shape is needed to maintain time resolvability.

The ideal threshhold circuit is one that gives an output of the same shape when a given level is reached or exceeded, and gives no output when the given level is not exceeded. Combining these prerequisites with the 0.1 μ second time resolvability presents a difficult design problem. The unique parameters of the tunnel diode, however, provided a perfect solution. Combining a definite firing current, and a definite voltage pulse when that current is reached, provided an excellent threshhold. And, since the tunnel diode reacts in less than 10 nano-sec., all criteria were obtained. The resulting pulse output is > 100 volts, < 0.1 μ second. Again a cathode follower is used to give a low impedence output. The final circuit diagram is shown in Fig. 8.

3.10 The Timing and Display Units

The design of our data presentation system evolved from the basic ideas about the backscatter measurement that we expressed in our previous report (March 1966) and in the Introduction of the present report. Namely, given the atmospheric density at an altitude of 80 km, or a hypothetical dust layer, containing 10 particles per cubic meter, of a radius of one micron, at a height of 100 km, it would be necessary to add together - interval by interval - a few thousand shots, in order to obtain, in every resolution interval of 1.5 km, a backscatter measurement equal to at least 10 times its fluctuation.

This implies two basic requirements: a presentation system that will display signal pulses on a time scale suitable for counting pulses in 10 micro-second intervals (1.5 km); and an integration system capable of superimposing many

successive presentations. The answer that comes naturally to mind is a cathode-ray tube display with, say, negative-going range pips and positive-going signal pulses, and a photographic recorder that will superimpose many scans on the same frame.

During high altitude observations, very few signal pulses will appear on the display. The Tables included in pages 18 and 22 of our previous semi-annual report (March 1966) indicate that the hypothetical dust layer should yield about 2 pulses per range interval every 100 scans, while molecular backscatter from an altitude of 80 km would yield about 10 pulses per range interval over 100 scans. In view of these numbers, it was decided to present our range on a scale of 1 cm per range interval. The situation changes, however, at low altitudes. Our previous work shows that, from a height of 20 km, we would obtain from gas molecules alone, about 7500 pulses per range increment in one single scan. Which, in turn, implies that we would have to add a neutral filter into the optical receiver in order to make the signal manageable. In other words, high and low altitude observations will not be carried out simultaneously, which is also in accord with the fact that, in general, they arise from different interests.

This establishes another basic point in our design: the complete range from the surface to 150 km altitude can be divided into several smaller ranges, that we call "modes" in our instrument, and that are selectable by means of appropriate switches. Although they are meant to cover different regions of the atmosphere, they are made to overlap in order to allow for comparison between them. There are five such modes, as shown in the following table:

Mode	From Altitude	To Altitude	Scale Factor
I	60 km	150 km	1 cm per interval
II	30 km	75 km	1 cm per interval
III	15 km	37.5 km	3 cm per interval
IV	7.5 km	15 km	15 cm per interval
V	0	10 km	15 cm per interval

In order to achieve the above-mentioned scale, a 7" cathode-ray tube was used to build the display. On this tube, however, the whole timebase for every mode would still be much greater than the screen diameter and, so, had to be displayed in raster form.

However, a common problem with rasters is the dead time between individual traces, while the electron beam returns to the left edge of the screen. In order to eliminate this dead time, we built a special time-base generator, that scans successive traces in alternately opposite sense, and a very fast step generator, that lowers the beam at the end of each trace. Both circuits are described below.

Negative-going timing pips are now added to the trace, one short pip every ten microseconds (one range interval) and one longer pip every 50 microseconds. Signal pulses are presented in positive polarity on the trace. The timing pulses in question are the controlling elements for the timebase itself and, so, the accuracy and stability of the whole unit depend only and entirely on the accuracy and stability of the timing oscillator, from which everything else is derived.

That the unit is quite stable enough for integration of hundred scans over one frame (which, with our laser firing once per second would take less than two minutes) is clearly shown in Fig. 9. This is a one-minute exposure of our time-base and range scale, repetitively triggered 300 times per second; there are, then, 18,000 scans superimposed in that photograph.

It must be pointed out that, during integration, the brightness of the trace and range pips must be kept very low, to avoid fogging the picture. On the other hand, signal pulses must be clearly recorded upon a single appearance and, therefore, require higher brightness level. This is solved by applying signal pulses to the deflection plates and brightening grid at the same time, thus enhancing the brilliance for the duration of each signal pulse.

At present, the 30 tube timing unit is completed and fully operational, although some of its circuits are being fed with laboratory power supplies. The display, on the other hand, is under assembly, and some of the power supplies for both units still have to be constructed.

3.11 Operation of the Timing Unit

The action can be described with reference to the simplified block diagram in Fig. 10. A main trigger pulse is received from the photodiode following the laser (see Section 3.1), and starts the generation of the main gate, a negative rectangle starting at time zero and lasting somewhat longer than necessary for the maximum range in use. Its generator is a conventional flip-flop as shown in the circuit (Fig. 11). The blocking oscillator shown on the same diagram generates a resetting pulse for some of the circuits, at the end of the main gate.

The main gate starts the 10 microsecond marker generator shown in Figure 10. This block is the timing reference of the whole system. It consists of the pulsed 100 Kc oscillator shown in Fig. 12 - a ringing circuit with capacitive cathode-load feedback - and the comparator shown in Fig. 13. The latter is of the family of the "long-tailed pair" and triggers a blocking oscillator, whose output is a train of 45 v positive pulses, of 0.4 microsecond width at their base and spaced at 10 microsecond intervals; this train lasts as long as the main gate.

As for the stability of the ringing circuit, it was extensively tested during the last six months and displayed excellent long-term stability and very little jitter. No measurable frequency change occurred upon variation of the heater voltage between 5.7 v and 6.9 v, the positive 300 v supply between 285 v and 315 v or the negative supply between -190 v and -210 v (nominal value: - 200 v), nor between changes in the last two in combination. The amplitude change never exceeded 5% during the heater test or 10% during the DC tests, except for the first two cycles.

The next unit shown in Fig. 10 is the 50 microsecond marker generator, which consists of a flip-flop divider by 5 and a blocking oscillator, as shown in Fig. 14. The output of the latter is a train of positive 55 v pulses, of 0.5 microsecond width and coincident with every fifth 10 microsecond marker. In addition to a timing function that will be explained later, they are meant to make it easier to read the range scale, and to that end, they are made greater than the 10 microsecond markers.

The delay gate shown next on Fig. 10 is a digital counter that selects an appropriate marker to trigger the following stage or the timebase generator, depending on the mode in use. The counter is made of three monostable multivibrators with very long metastable states, which means that they automatically reset themselves to zero a few hundred microseconds after the complete scan is over. The circuit diagram appears in Fig. 15. Since the output can be taken from the first, second, or third stage, the unit can count the second, fourth, or eighth 50 microsecond marker, which is then used to trigger another flip-flop, which generates a gate pulse of long duration. This is applied to the suppressor of a 6AS6 pentode whose grid receives either the 50 microsecond markers or the 10 microsecond markers, depending on the mode. In mode V, the delay gate is not used at all.

The following subunit, labelled 150 microsecond trigger generator in Fig. 10, is a divider by 3 otherwise similar to the 50 microsecond marker generator. It is used in modes I and II only; it operates on the gated train of 50 microsecond markers and produces trigger pulses for the time-base at 150 microsecond intervals. Figure 16 shows the circuit.

Figure 17 shows the circuit of the timebase generator, which is a rather humorous combination of two well-known configurations. The problem at hand is to generate a bi-directional time-base and is solved in straightforward fashion. V24 is coupled to a resistor chain by a capacitor of 0.1 microfarad. These elements form a bootstrap circuit which generates a linear rising ramp. The action is started by one trigger pulse and stopped by the next, by means of

multivibrator V22. The aforementioned capacitor then must discharge, which it would, exponentially, through V23. This pentode, however, is connected as a Miller integrator, and therefore responds with a linear descending ramp at its plate. The duration of the sweep is, of course, varied by switching condensers, and two independent adjustments are provided for the positive and the negative slope.

Thus, the time-base. It now remains to step the vertical deflection voltage in discrete steps at the extremes of each horizontal trace. A staircase generator seems the obvious choice but, in order to count all events from the photomultiplier, each vertical step (the riser on a staircase function) should be of less than 0.1 microsecond duration. The tunnel diode was chosen as the active device due to its speed. And, as the tunnel diode is a current device, the only remaining requirement was some method to switch the current from tunnel diode to tunnel diode to allow a train of pulses to give a staircase. The transistors, shown in Fig. 18, accomplish this. Normally, the upper tunnel diode has about 5% less than peak current flowing through it. When the first pulse comes along, it switches, turning on the transistor connected across it. This gives the first step in the staircase, and switches enough current to the second tunnel diode that it now has about 5% less than peak current flowing through it. The action continues until the last tunnel diode switches. The circuit is reset by clamping the staircase voltage to zero.

This completes the description of the timing unit, except for a few minor circuits that serve auxiliary functions and need not be discussed here. It may be useful, however, to sketch some waveforms in the various modes. This is done in Fig. 19, where time and range scales appear at the top, followed by both trains of timing markers. The delayed gate is then shown for every mode except mode V, for which the main gate is shown. Under every gate, the duration of the time-base is indicated by a horizontal line, and the triggers used to synchronize the traces are superimposed on it.

4. Project Time Schedule

Our time schedule is best presented by means of the diagram, Figure 20, which is divided as follows:

Section 1	shows the University contribution to the project.
Section 2	applies to the transmitting equipment.
Section 3	covers the optical and electronic receiving units.
Section 4	contains the timing, displaying, and recording gear.
Section 5	indicates tests that must be made before the experiment.
Section 6	shows the experiment proper.
Section 7	indicates when reports are due.

It will be seen that, whereas most of the system should be ready towards the end of January, the high-speed shutters will probably take longer, whence our suggestion, in Section 3.5, that we might begin the observational phase of the program with provisional shutters of another kind.

Also, it was hoped to start testing the photomultiplier in December. Unfortunately, however, the tube broke and we are now awaiting replacement.

5. Detail of the University Support to the Program

A well-equipped laboratory was set up during the past year, out of University funds, in support of this program. Photographs of the facilities are included in the report.

The considerable amount of electronic work done last summer would not have been possible otherwise, as will readily be understood from the list of instruments presently available:

Oscilloscope
Hewlett Packard Model #422
Test Oscillator
Hewlett Packard Model #651A
Electronic Counter
Hewlett Packard Model #5244L
Pulse Generator
General Radio Model #1398A

As a result of purchases made for other research grants and contracts, the following equipment is also available in the optics laboratory for use on this program:

Perkin-Elmer Helium Neon Laser Model #5300
8 mw output power in fundamental mode (6328 Å) with output beam diameter of 3 mm and divergence of 0.3 mo.
Ealing Two Meter Optical Bench
with accessories including: lens holders, carriers with vertical or horizontal micrometer adjustment, collimator, adjustable slit, adjustable aperture, etc.
Control Instrument Company, 10" Telescope
Cassegrain optical system of 120" focal length.
A variety of high-quality photographic equipment including:
Graflex and Polaroid cameras and accessories.

In addition to these, purchased last spring, a Hewlett Packard oscilloscope Model #547 was already in our lab, as well as a Hewlett Packard 212A

pulse generator and an abundant assortment of VT voltmeters, power supplies, tube and transistor testers, impedance bridges, etc.

Incorporated as part of our electronics is a machine shop equipped with basic power tools such as drill press, rotary table, grinder, precision lathe, and all necessary hand tools.

The laboratory was staffed with one full-time technician at the beginning of the year and another since July; in addition, part-time and student technicians have contributed to the development of the equipment.

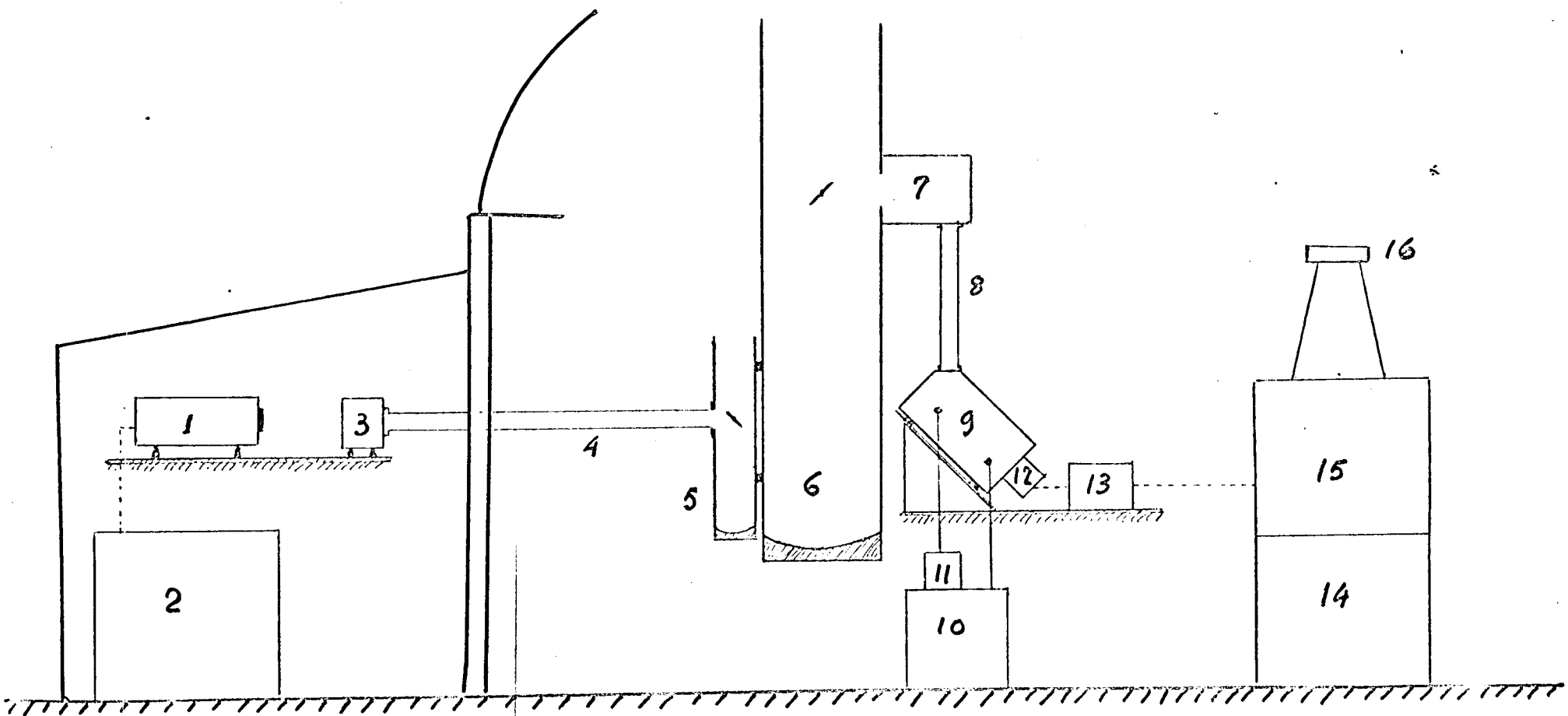

Fig 1.- System Layout

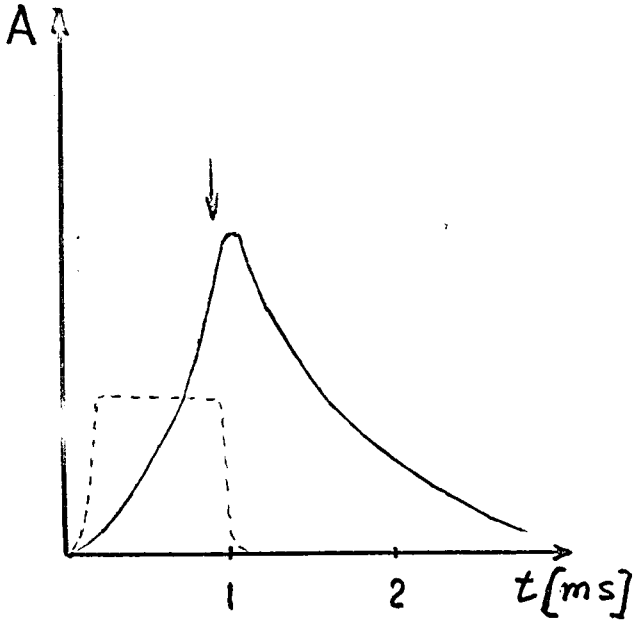

Fig 2.- Pulse timing

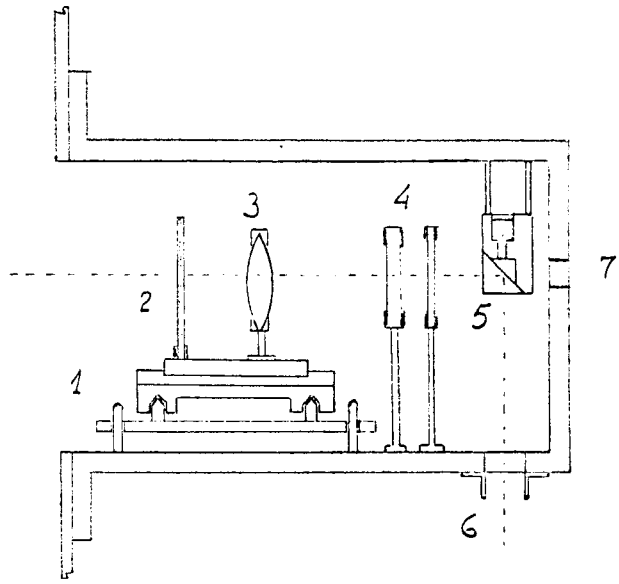

Fig. 3.- Optical Receiver

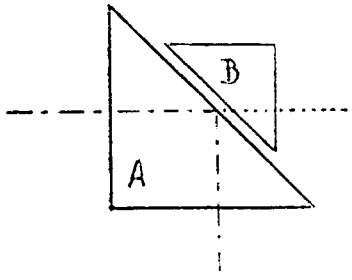

Fig. 4.- Frustrated Reflexion

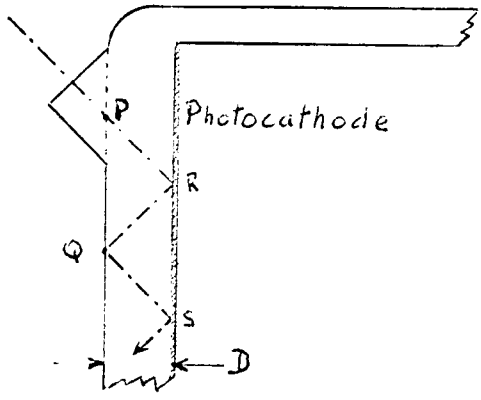

Fig. 5 - Internal Reflexion in Window

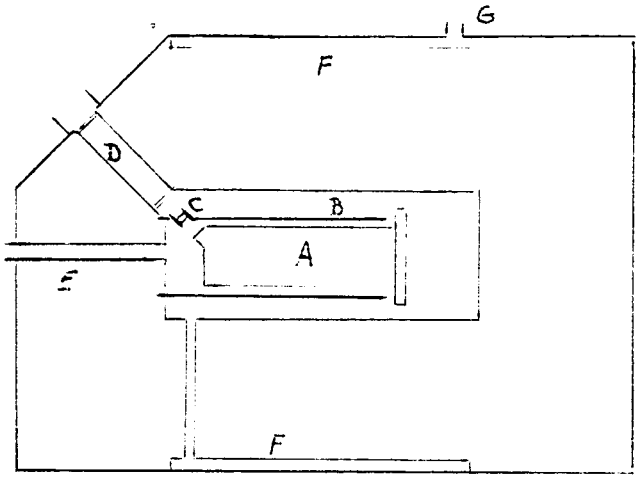

Fig. 6. - Detector Housing

PREAMP.

RBW
11-18-66

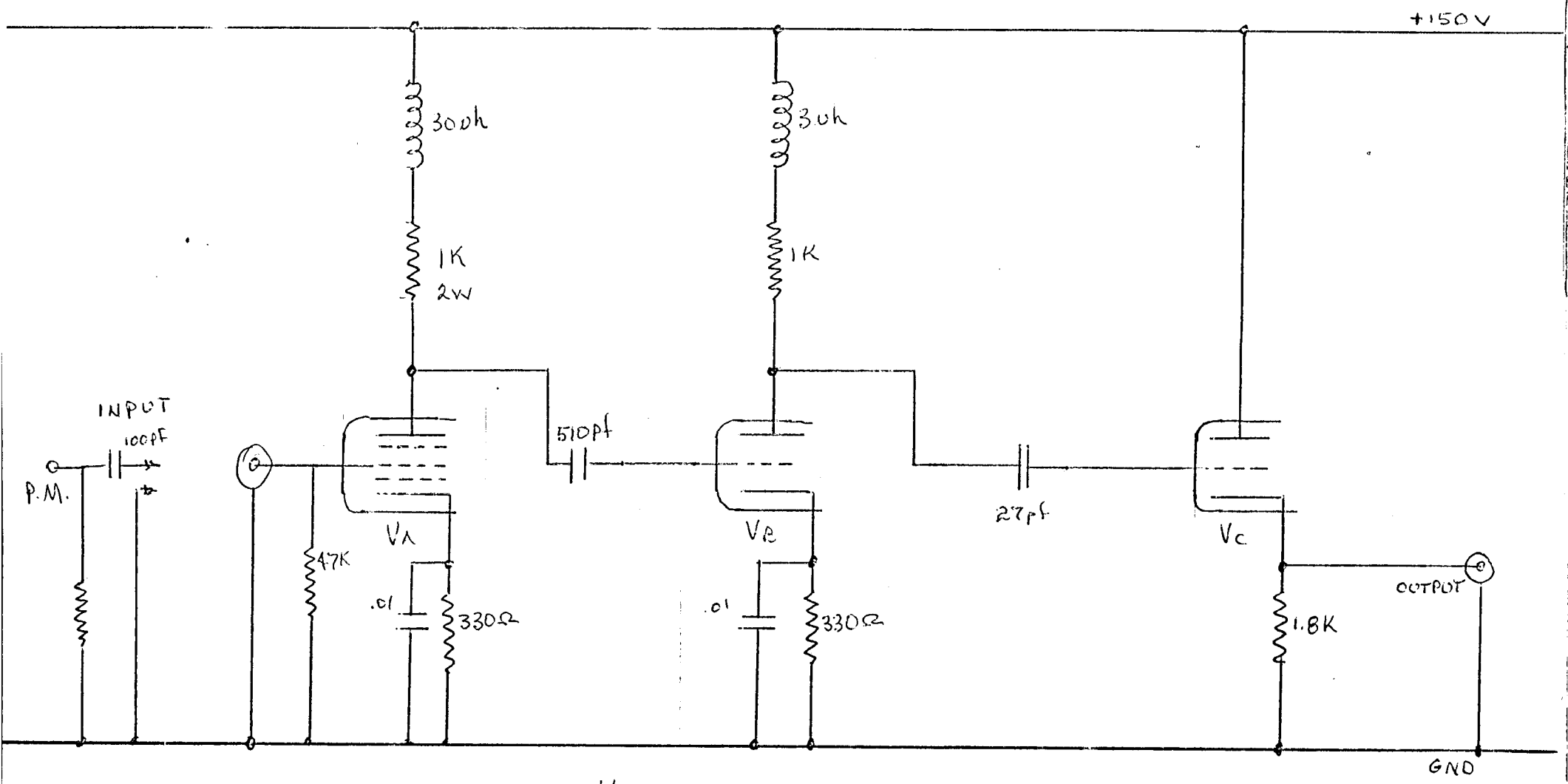

V_{A8C} - 6AF'1

Fig. 7

VIDEO AMP.
(AND PULSE DISCRIMINATOR)

R.B.W.
11/18/66

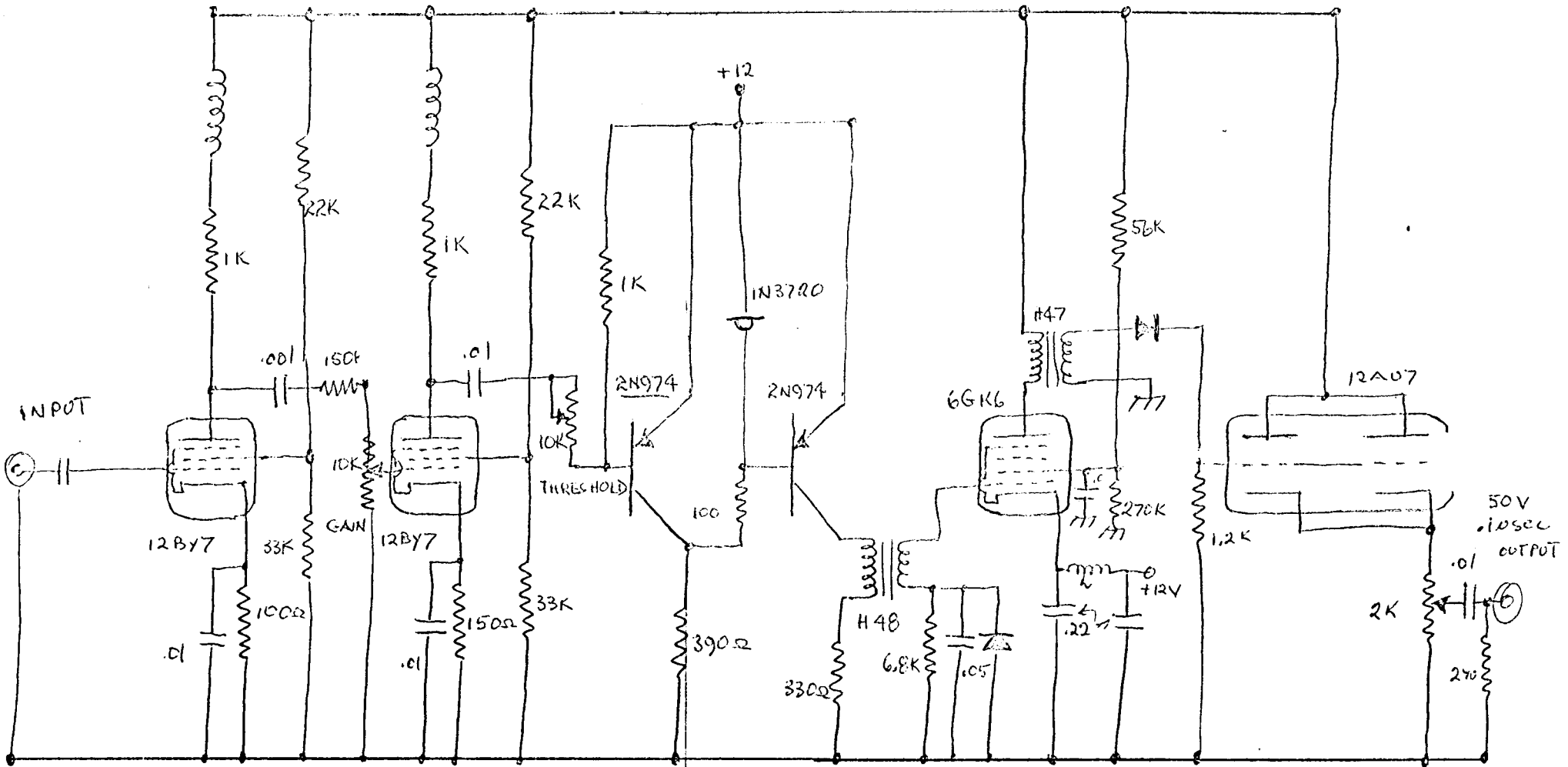

Fig. 8

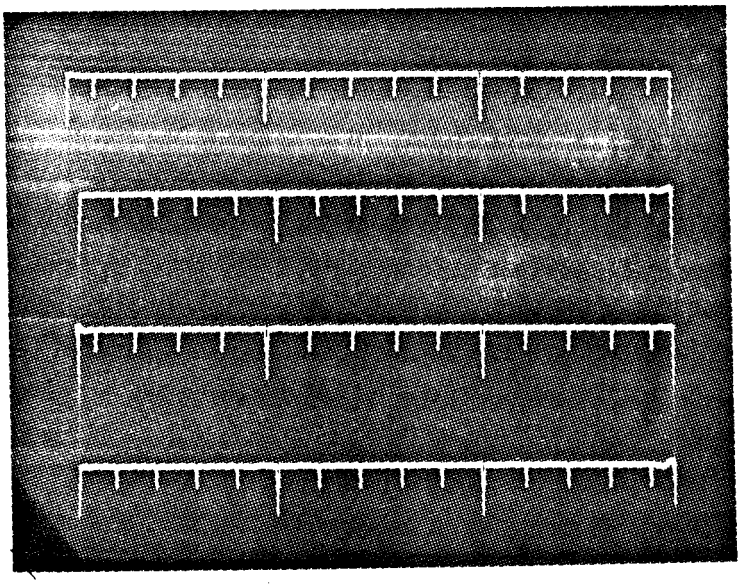

Superposition of 18,000 scans of timebase in Mode 5

Fig. 9

TIMING UNIT - BLOCK DIAGRAM

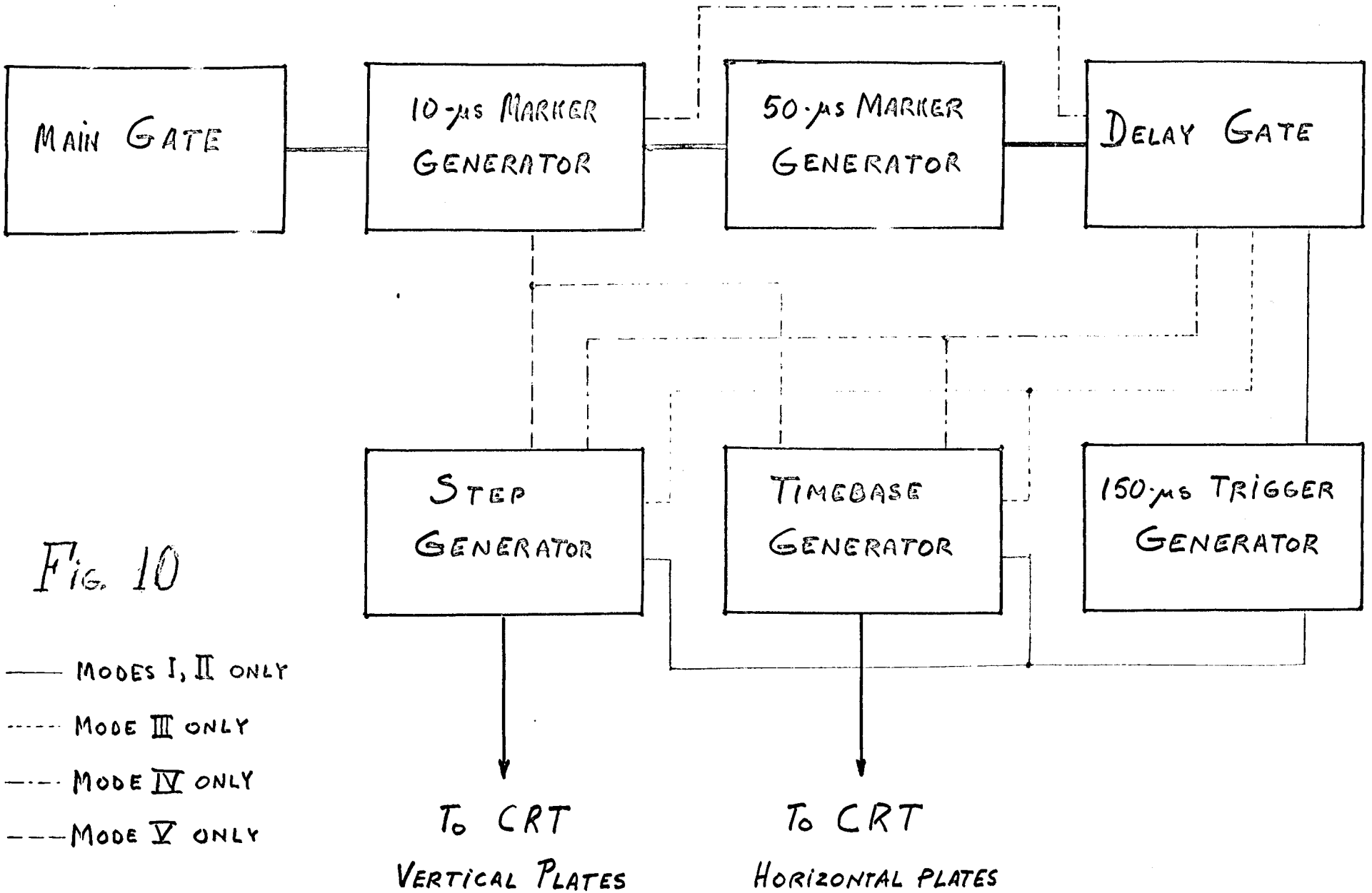

FIG. 10

MAIN GATE (MODIFIED)

RBW
11/18/66

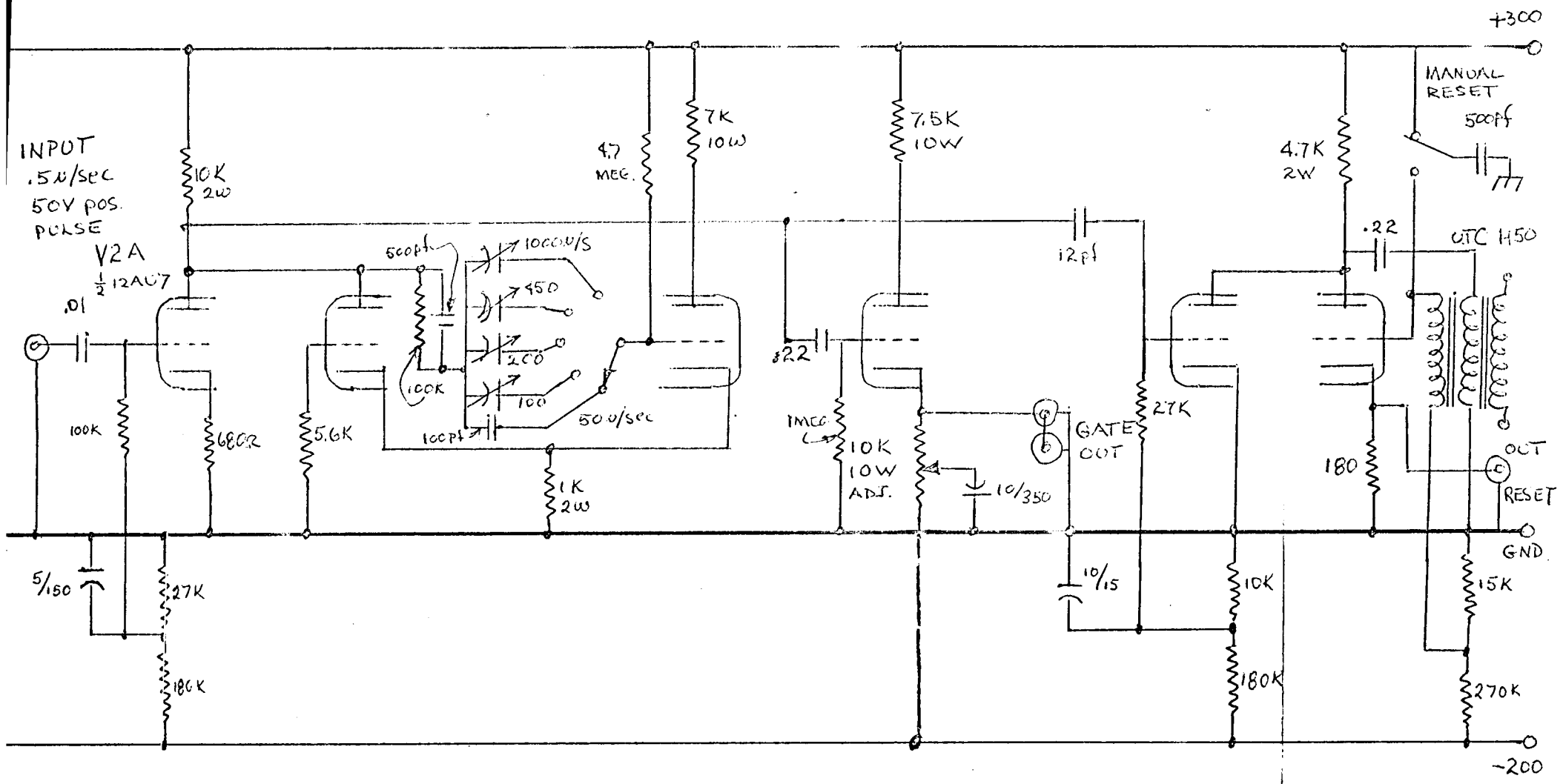

Fig 11

100 KHz
PULSED O[illegible].
(MODIFIED)

RBW
11/18/66

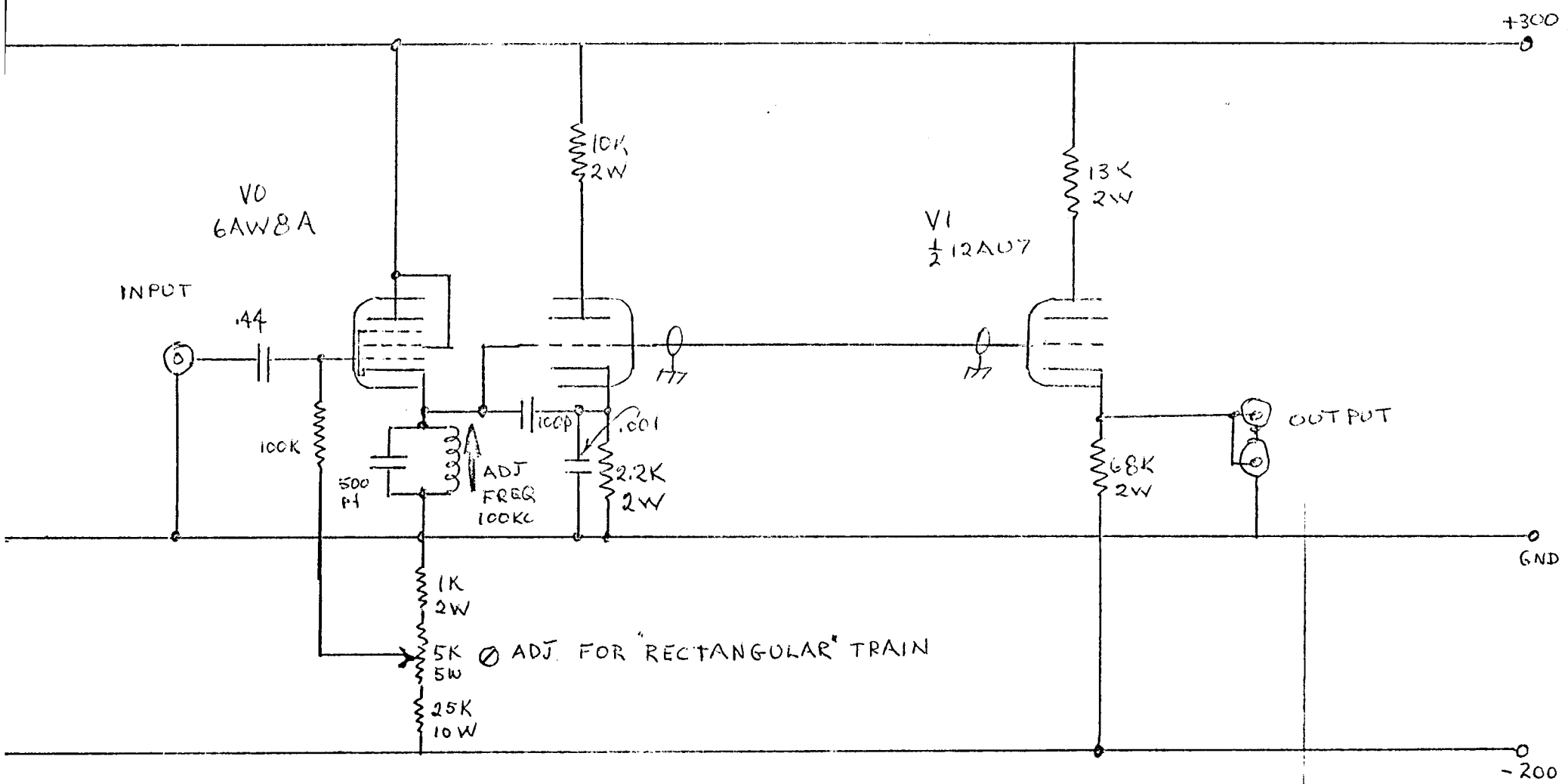

Fig. 12

COMPARATOR

5/9/66

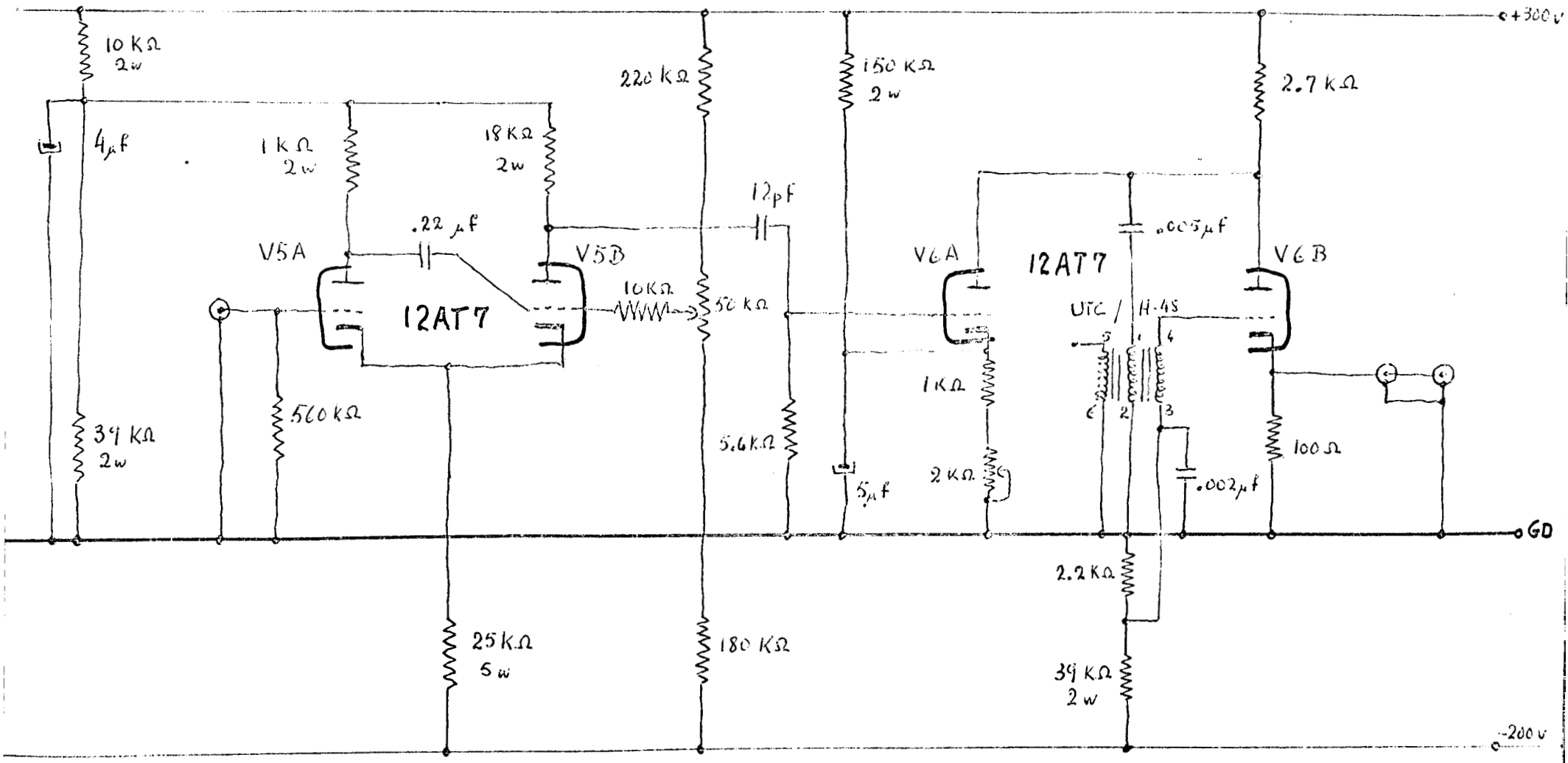

Fig. 13

1:5 Divider

5/13/66

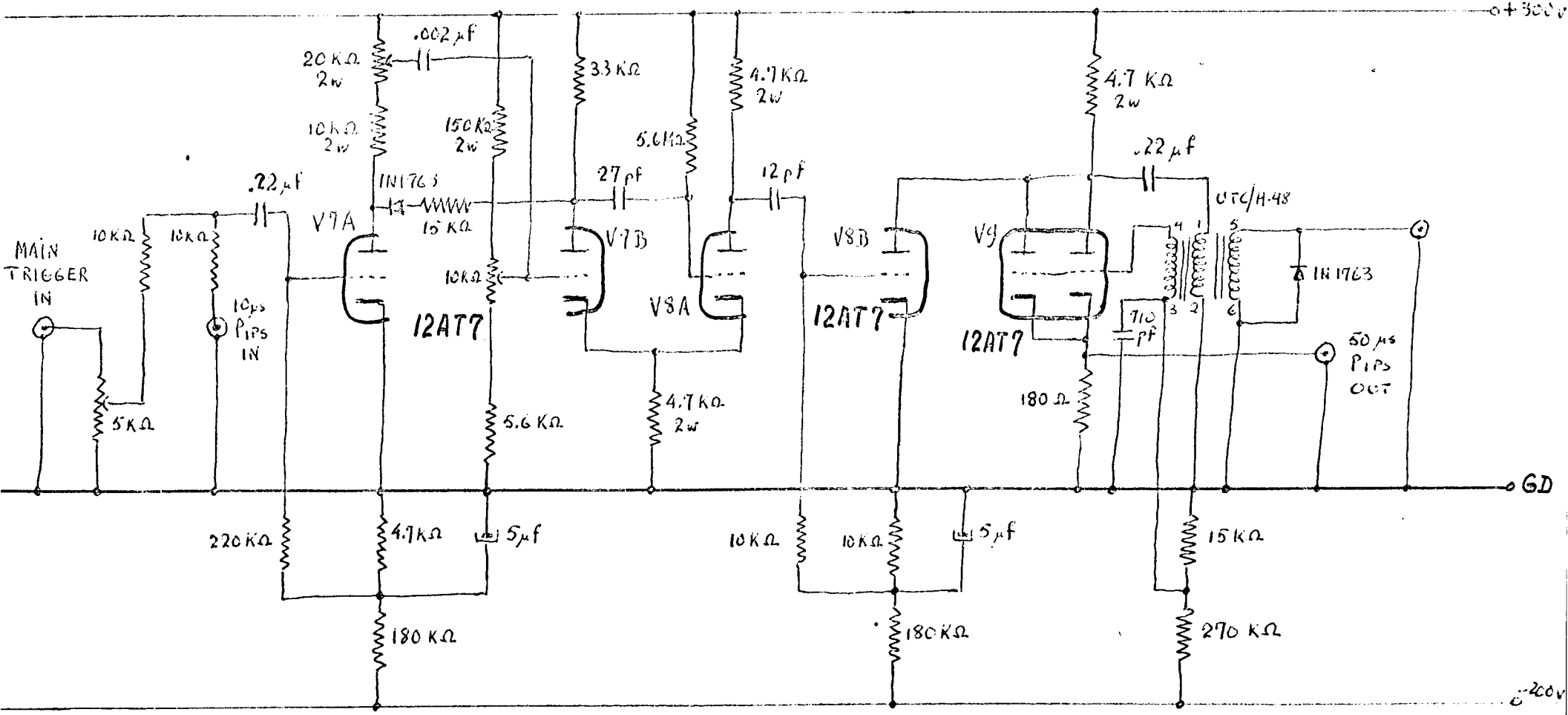

Fig. 14

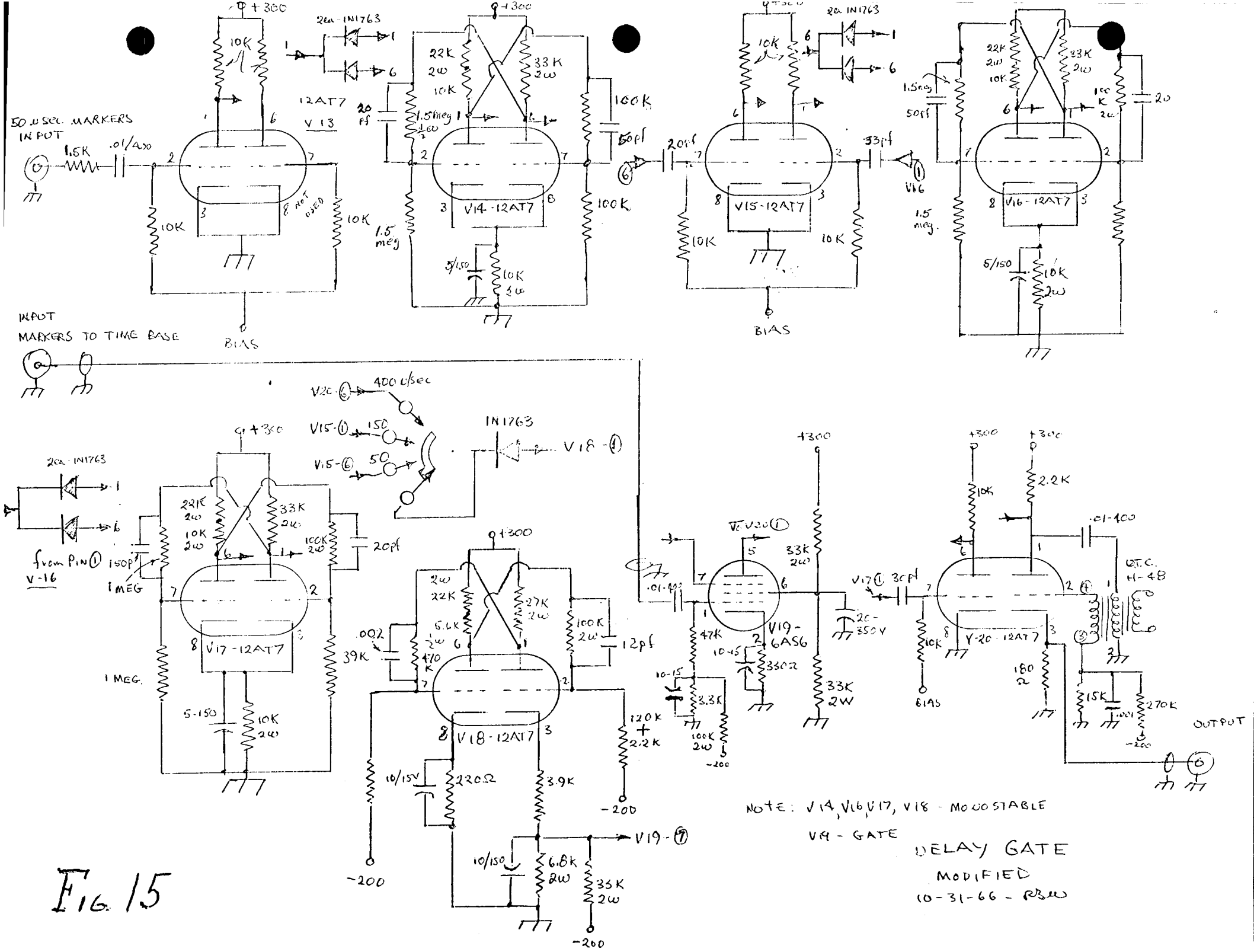
50 μ SEC. MARKERS
INPUT
1.5K
.01/400
10K
12AT7
V 13
2ea - IN1763
22K 2W
10K
33K 2W
20 pf
1.5meg
100K
50pf
V14 - 12AT7
5/150
10K 3W
1.5 meg
20pf
33pf
V15 - 12AT7
V16
1.5meg
50pf
22K 2W 10K
33K 2W
100K 2W
20
V16 - 12AT7
5/150
10K 2W
INPUT
MARKERS TO TIME BASE
BIAS
V20 - ⑥ 400 c/sec
V15 - ① 150
V15 - ⑤ 50
IN1763
V18 - ①
2ea - IN1763
from PIN ① V-16
150pf
1 MEG
22K 2W
10K 2W
33K 2W
100K 2W
20pf
V17 - 12AT7
5-150
10K 2W
1 MEG.
.002
39K
2W 22K
5.6K 1/2W
470K
27K 2W
100K 2W
12pf
V18 - 12AT7
10/15V
220Ω
3.9K
120K
2.2K
-200
10/150
6.8K 2W
33K 2W
V19 - ⑦
V19 - 6AS6
V20 ①
33K 2W
47K
10-15
3300Ω
3.3K
100K 2W
20 - 350V
V17 ① 30pf
10K
2.2K
.01-400
V-20 - 12AT7
180 Ω
15K
270K
U.T.C. H-48
OUTPUT
NOTE: V14, V16, V17, V18 - MONOSTABLE
V19 - GATE
DELAY GATE
MODIFIED
10-31-66 - RBW

Fig 15

1:3 Divider

1/6/66

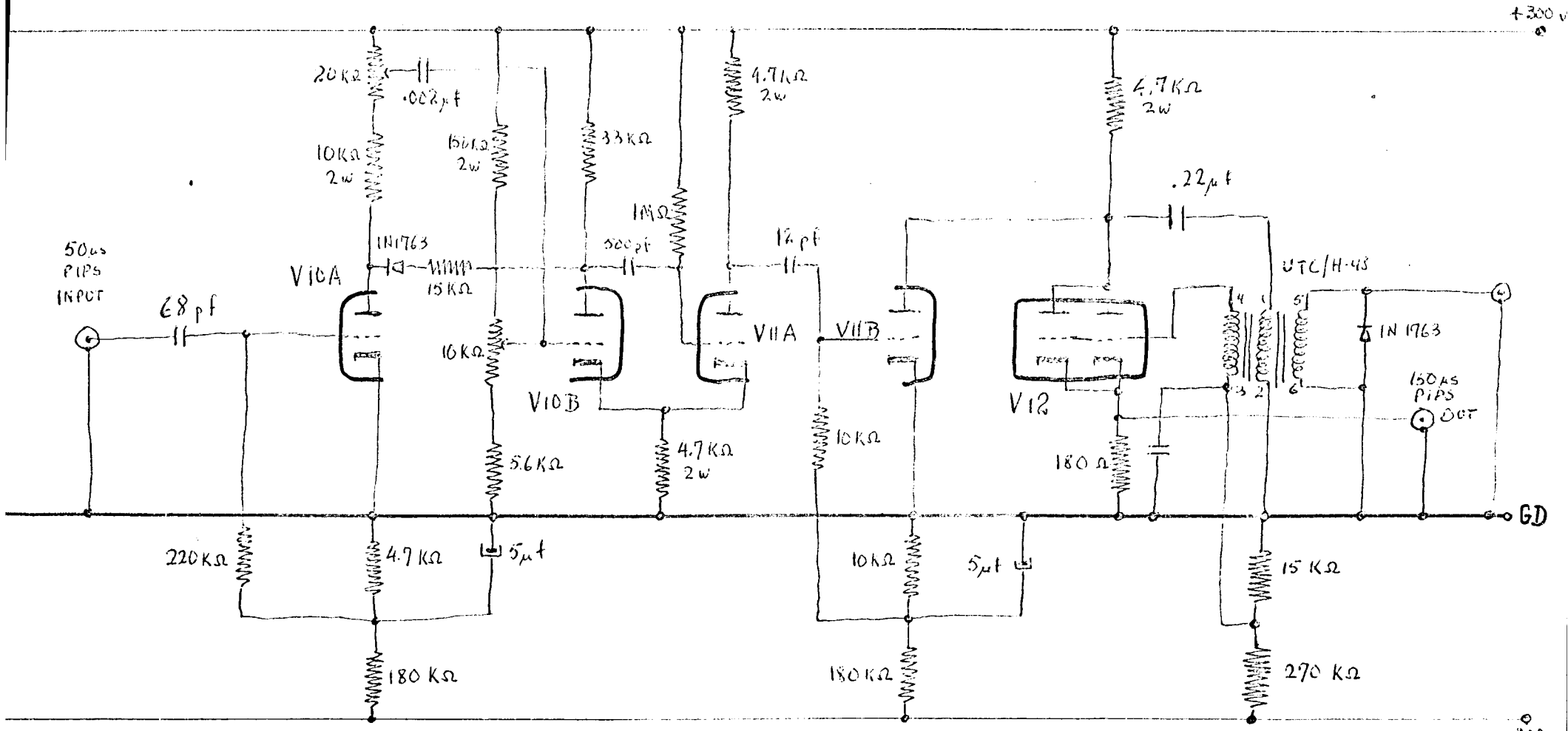

Fig. 16

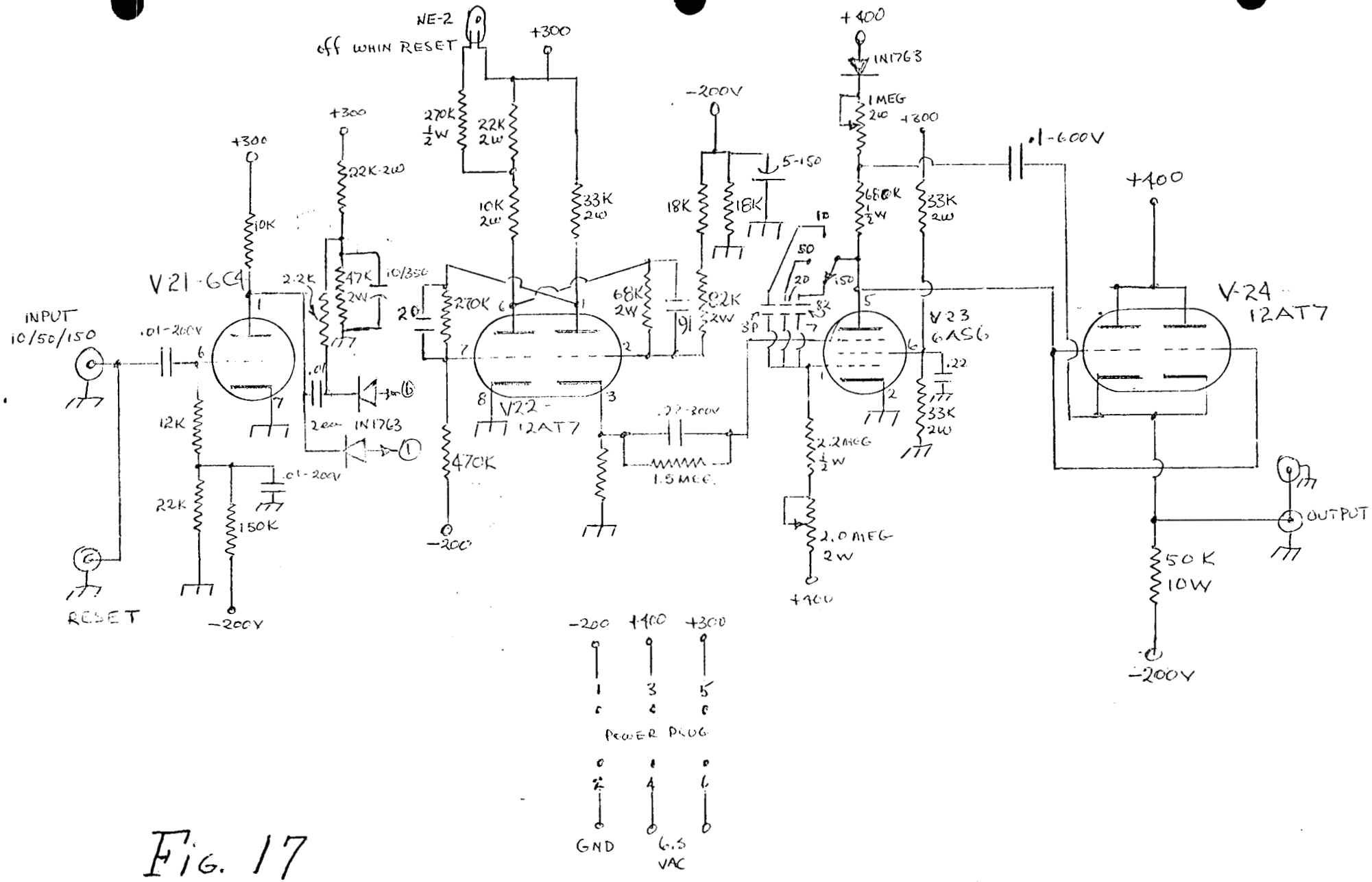

Fig. 17

TIME BASE GENERATOR
MODIFIED
11-2-66 - RBW

STEP GEN.

R.B.W.
11-18-66

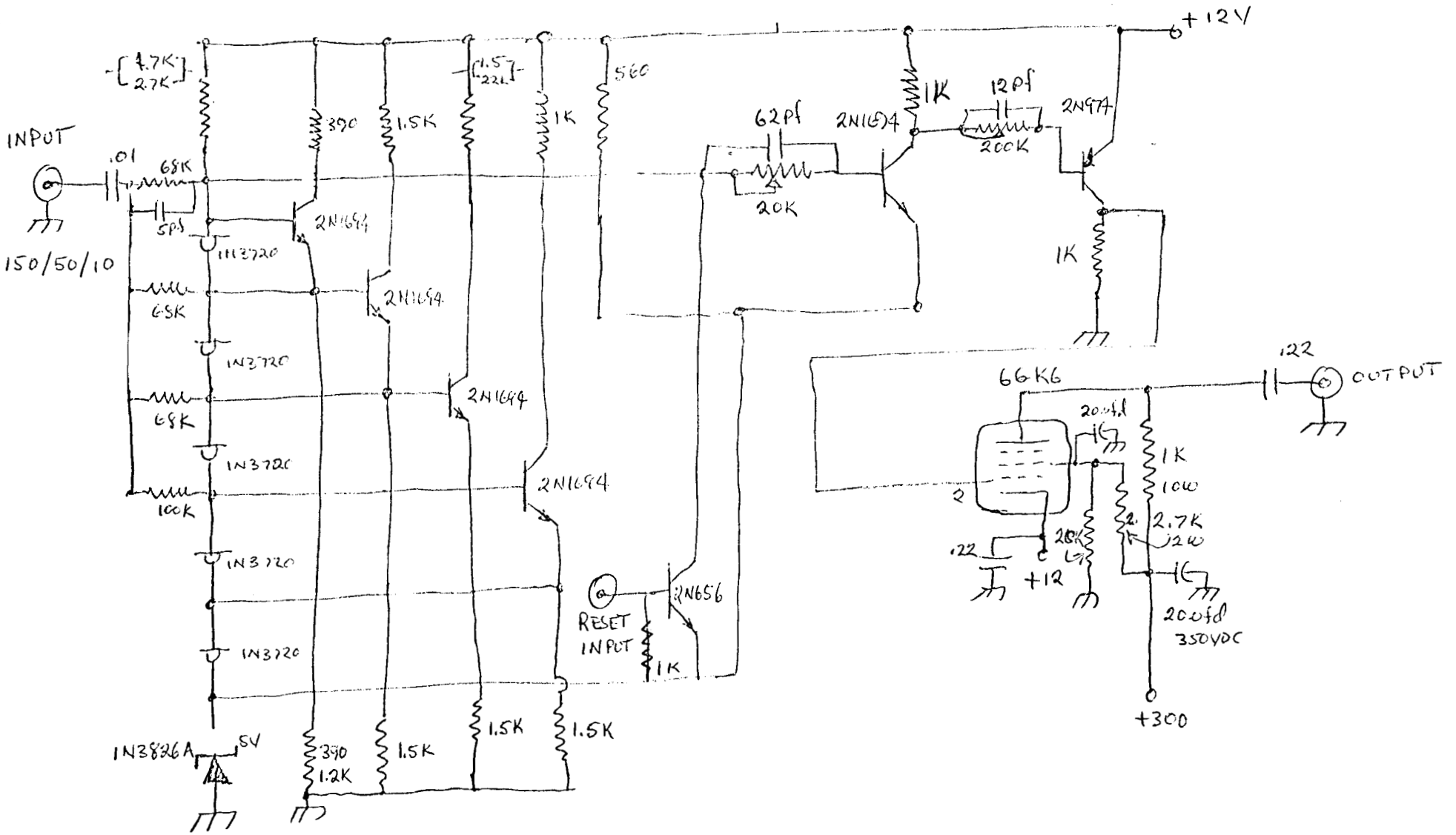

Fig. 18

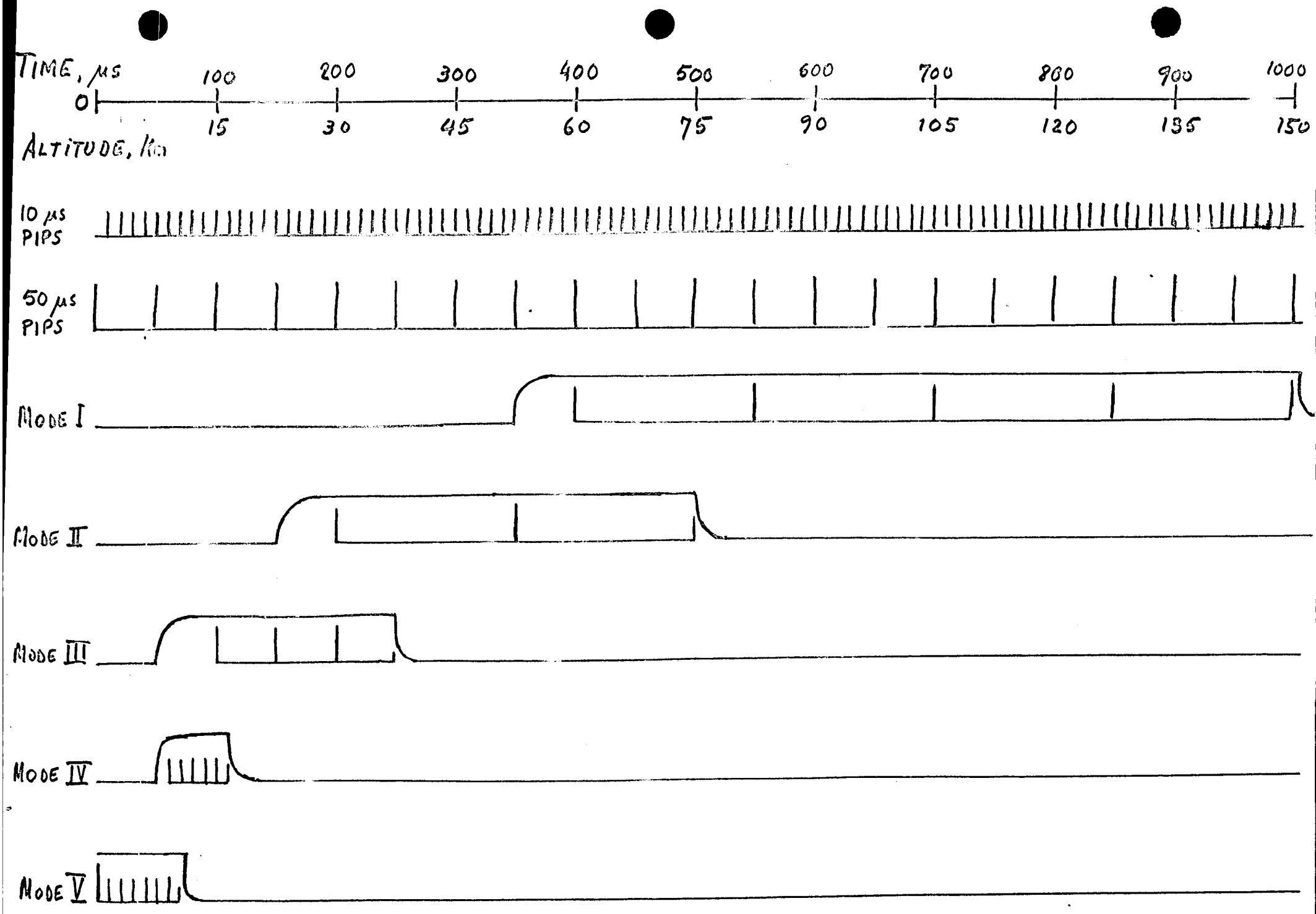

FIG 19.- PULSE RELATIONS IN VARIOUS MODES

UNIVERSITY OF MIAMI. LASER SOUNDER PROGRAM. NASA GRANT NGR-10-00[illegible]28, SUP. #1

Development or Procurement

Building & Testing

Ready

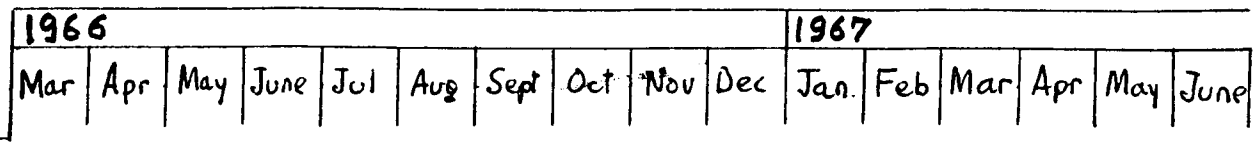

University Capital Procurement - $ 10,000.-

Laser & Power Supply

Fluorescence Shutter

Transmitting Telescope

Receiving Telescope & Facilities

Optical Receiver (except Shutter)

Receiver Shutter

Detector - Efficiency Improvement.

Detector Housing & Cooling System

Preamplifier

Video Amplifier

Timing Unit

Display Unit

Photographic Recorder

Dark Current Tests. (Replacement of Photomultiplier)

Sky Background Measurements

BACKSCATTER EXPERIMENT

REPORTS

FIG. 20

* *